Optimal estimation of rain rate profiles from single-frequency radar echoes

Ziad S. Haddad
Eastwood Im
Steve Durden

Jet Propulsion Laboratory, California Institute of Technology

Abstract

The significant ambiguities inherent in the determination of a particular vertical rain intensity profile from a given time profile of radar echo powers measured by a downward-looking (spaceborne or airborne) radar at a single attenuating frequency are well-documented. Indeed, one already knows that by appropriately varying the parameters of the reflectivity-rain-rate ($Z-R$) and/or attenuation-rain-rate ($k-R$) relationships, one can produce several substantially different hypothetical rain rate profiles which would have the same radar power profile. Imposing the additional constraint that the path-averaged rain-rate be a given fixed number does reduce the ambiguities but falls far short of eliminating them. While we now know how to generate as many mutually ambiguous rain-rate profiles from a given profile of received radar reflectivities as we like, there remains to produce a quantitative measure to assess how likely each of these profiles is, what the appropriate "average" profile should be, and what the "variance" of these multiple solutions is. Of course, in order to do this, one needs to spell out the stochastic constraints that can allow us to make sense of the words "average" and "variance" in a mathematically rigorous way. Such a quantitative approach would be particularly well-suited for such systems as the proposed Precipitation Radar of the Tropical Rainfall Measuring Mission (TRMM). Indeed, one would then be able to use the radar reflectivities measured by the TRMM radar from one particular look in order to estimate the most likely rain-rate profile that would have produced the measurements, as well as the uncertainty in the estimated rain-rates as a function of range. Such an optimal approach is described in this paper.

1 Introduction

The Tropical Rainfall Measuring Mission (TRMM) precipitation radar will be the first of its kind to measure vertical rainfall distributions from space. The TRMM radar will scan across the nadir track using a single (13.8 GHz) frequency. The range-gated backscattered powers over the entire scan swath will be measured, averaged, and processed to derive the rainfall rates. The fact that the data will consist of measured effective reflectivities at a single attenuating wavelength implies that the rain-rate retrieval problem will have multiple solutions. This inherent ambiguity would not pose a significant problem if the difference between these multiple solutions were known to be small in most cases. Unfortunately, the opposite is true (see [3], [5], [12], [6]). In fact, it was shown in [6] how, by appropriately varying the parameters of the reflectivity–rain-rate ($Z-R$) and attenuation–rain-rate ($k-R$) relationships, one can produce several substantially different hypothetical rain rate profiles which would have the same radar power profile. It turns out that even if one imposes the additional constraint that the path-averaged rain-rate be a given fixed number, the ambiguities are reduced somewhat but remain quite significant. While [6] shows how to generate a continuum of mutually ambiguous rain-rate profiles from a given profile of received radar reflectivities, there remains to produce a quantitative measure to assess how likely each of these profiles is, what the appropriate "average" profile should be, and what the "variance" of these multiple solutions is. Of course, in order to do this, one needs to spell out the stochastic constraints that can allow us to make sense of the words "average" and "variance" in a mathematically rigorous way.

In this paper, after summarizing the results of [6] concerning the extent of the ambiguity problem, we shall propose a stochastic framework to allow us to restate the problem above in exact mathematical terms, namely the problem of finding an appropriate "average" profile, and computing the "variance" of all the other profiles that could theoretically be solutions to the same inversion problem. We then derive an optimal approach to solve this problem by determining that rain-rate profile which, on average, best fits the radar measurements. We also quantify the effect that the ambiguities have on the rain-rate by calculating the uncertainty in the estimate, as a function of the measured data.

2 Ambiguities

To make this exposition self-contained, we summarize the results derived in [6] in this section, and we reproduce some of the examples. In order to approach the problem mathematically, one needs to model the dependence of the received power on the rain rate itself. In fact, the

effective reflectivity $p(r)$, measured from range r by a nadir-looking monostatic narrow-band radar such as TRMM, is proportional to the reflectivity coefficient Z of the rain at range r, and to the accumulated attenuation from range 0 to range r. Calling $k(r)$ (resp. $R(r)$) the attenuation coefficient (resp. rain rate) at range r, we begin with the simple empirical model that $Z = aR^b$ and $k = \alpha R^\beta$ for some value of the parameters a, b, α and β, and that the calibrated reflectivity is therefore given by

$$p(r) = C(r) \cdot aR(r)^b 10^{-0.2\alpha \int_0^r R(t)^\beta dt}, \tag{1}$$

where $C(r)$ represents the range-dependent calibration constant, which we assume to be known exactly. Since it is highly unlikely that a, b, α or β are ever known exactly, one would like to quantify the effect on R of an error in these parameters. Assuming that these parameters remain constant throughout the rain column it is shown in [6] that two different sets of rainfall parameters $\{R_0(r), a_0, b_0, \alpha_0, \beta_0\}$ and $\{R_1(r), a_1, b_1, \alpha_1, \beta_1\}$ give rise to the same effective reflectivity $p(r)$ exactly when

$$R_1(r) = \frac{R_0(r)^{b_0/b_1} 10^{-0.2\frac{\alpha_0}{b_1}\int_0^r R_0(t)^{\beta_0} dt} dr}{\left((a_1/a_0)^{\beta_1/b_1} - \frac{0.2\log(10)\alpha_1\beta_1}{b_1}\int_0^r R_0(r')^{b_0\beta_1/b_1} 10^{-0.2\frac{\alpha_0\beta_1}{b_1}\int_0^{r'} R_0(t)^{\beta_0} dt} dr'\right)^{1/\beta_1}}. \tag{2}$$

If, instead of using the directly measured effective reflectivities as our starting point, we use the surface-referenced data as in [11], i.e. if we divide $p(r)$ at every range r by $p(r_s)$, where r_s denotes the range to the surface, it is shown in [6] that two sets of rain parameters $\{R_0(r), a_0, b_0, \alpha_0, \beta_0, \sigma_0\}$ and $\{R_1(r), a_1, b_1, \alpha_1, \beta_1, \sigma_1\}$ (where σ denotes the surface backscattering coefficient) give rise to the same surface-referenced effective reflectivities if

$$R_1(r) = \frac{R_0(r)^{b_0/b_1} 10^{0.2\frac{\alpha_0}{b_1}\int_r^{r_s} R_0(t)^{\beta_0} dt}}{\left(\left(\frac{\sigma_0 a_1}{\sigma_1 a_0}\right)^{\beta_1/b_1} + \frac{0.2\log(10)\alpha_1\beta_1}{b_1}\int_r^{r_s} R_0(r')^{b_0\beta_1/b_1} 10^{0.2\frac{\alpha_0\beta_1}{b_1}\int_{r'}^{r_s} R_0(t)^{\beta_0} dt} dr'\right)^{1/\beta_1}}. \tag{3}$$

One can remove the assumption that the $Z - R$ and $k - R$ relations are constant throughout the rain column, and consider more physical relations by expressing Z, k and R directly in terms of the drop size distribution. Specifically, denoting by $\int_{D_-}^{D_+} N(D)\, dD$ the fraction of drops per unit volume whose diameter is between D_- and D_+, and, following Ulbrich ([13]), assuming that $N(D)$ is Γ-distributed, i.e. that

$$N(D) = \frac{D^{m-1} e^{-D/(\overline{D}/m)}}{\Gamma(m)(\overline{D}/m)^m}, \quad 0 < D < \infty \tag{4}$$

with the distribution curvature parameter m and the mean drop size $\overline{D}$ to be determined, it is shown in [6] that two sets of rain parameters $\{R_0(r), m_0(r), \overline{D}_0(r)\}$ and $\{R_1(r), m_1(r), \overline{D}_1(r)\}$ give rise to the same effective reflectivities if

$$R_1(r) = R_0(r) \frac{\left(\frac{m_1(r)\overline{D}_0(r)}{m_0(r)\overline{D}_1(r)}\right)^{0.6} F(r)\, 10^{-0.2\int_0^r k_0(t)\,dt}}{F(r)\, 10^{-0.2\int_0^r k_0(t)\,dt} + (1 - F(0)) - \int_0^r F'(t)\, 10^{-0.2\int_0^t k_0(\tau)\,d\tau}\, dt} \qquad (5)$$

where $F(r) = \frac{\Gamma(m_0(r)+6)\Gamma(m_1(r)+4.27)}{\Gamma(m_1(r)+6)\Gamma(m_0(r)+4.27)} \left(\frac{m_1(r)\overline{D}_0(r)}{m_0(r)\overline{D}_1(r)}\right)^{1.73}$, $F'(r)$ denotes the derivative of F with respect to r, and $k_0(r) = 0.026 \frac{\Gamma(m_0(r)+4.27)}{\Gamma(m_0(r)+3.67)} \left(\frac{\overline{D}_0(r)}{m_0(r)}\right)^{0.6} R_0(r)$ is the attenuation coefficient for the 0^{th} profile.

The most striking resemblence between equations (2), (3) and (5) is the fact that the ambiguities contribute exponentially with range. In fact, by varying the (many) parameters in these equations, one can easily produce substantially different rain profiles that would give the same data. We illustrate this effect by considering a constant rain rate profile $R_0 = 20$ mm/hr, and using the equations to compute profiles that would have produced the same measurements. For simplicity, we shall assume that the rain parameters are constant. Since they are not likely to remain constant over long segments of the rain column, we restrict our attention to ranges between $r = 0$ and $r = 3$ km.

To illustrate the case where surface-referenced effective reflectivities are used, we consider the two cases where

1) $\alpha_0 = 0.02$, $\alpha_1 = 0.03$, $\beta_0 = 0.98$, $\beta_1 = 1.08$, $b_0 = 1.4$, and $\sigma_0/\sigma_1 = 1.5\, a_0/a_1$.

2) $\alpha_0 = 0.03$, $\alpha_1 = 0.02$, $\beta_0 = 1.08$, $\beta_1 = 0.98$, $b_0 = 1.6$, and $\sigma_0/\sigma_1 = 0.75\, a_0/a_1$.

Figure 1 shows the two corresponding profiles, obtained using equation (3). Assuming that the parameter a is known exactly (i.e. that $a_0 = a_1$), these two cases show how a relatively small error in the value of the surface backscattering coefficient σ can lead to significantly different derived rain rate profiles. Indeed, in the first case, a 1.7 dB decrease in σ_0 (which corresponds to $\sigma_0/\sigma_1 = 1.5$), along with small changes in the remaining parameters, can result in an underestimate R_1 of the true rain rate $R_0 = 20$ that is off by $R_0/R_1 \simeq 1.66$, or about 66 %. Yet, in this case, the total path-integrated attenuation is 1.13 dB for the 0^{th} profile, and 0.98 dB for R_1, showing no exploitable difference. Similarly, the second case shows that increasing σ_0 by 1.2 dB (so that $\sigma_0/\sigma_1 = 0.75$), along with small changes in the other parameters, can produce an overestimate of the rain rate R_0 which is off by close to $R_1/R_0 \simeq 1.85$, or about 85 %. Allowing for uncertainties in the parameter a only aggravates the ambiguity.

To illustrate the case where the drop-size-distribution model is used with the directly measured effective reflectivities, we keep the constant profile $R_0 = 20$ mm/hr, and examine the following two cases:

3) $m_0 = 4$, $\overline{D}_0 = 1.5$, $m_1 = 2$, $\overline{D}_1 = 1$.

4) $m_0 = 2$, $\overline{D}_0 = 2$, $m_1 = 4$, $\overline{D}_1 = 1.5$.

Figure 2 shows the graphs of R_1 in each of these two cases, as given by equation (5). Again in this case, the path-integrated attenuation for the two profiles is not significantly different: an additional attenuation measurement would not be sufficient to distinguish between these two cases.

Before considering solutions to this problem, we note one additional important implication of the ambiguities problem, namely that one should be very careful in evaluating the performance of any particular rain-retrieval algorithm. Indeed, the conventional method of postulating a profile, simulating the resulting echo power data, running them through the algorithm of interest, then comparing its estimate with the original profile seems less than satisfactory, once one realizes that the particular data used could have been produced by a continuum of rain profiles, and that, therefore, the fact that one's algorithm can select one of these profiles (rather than any of the other, a priori equally possible, ones) is not in itself a measure of good performance. A sensitivity analysis of the algorithm at hand does not suffice to measure the accuracy of the algorithm, either. Heuristically, a sensitivity analysis only measures how "sure" the algorithm thinks it is of its answer, rather than how "correct" the answer is. Expressing these concerns in more rigorous terms is difficult as long as the rain retrieval problem remains a deterministic one: indeed, in the deterministic case, we know (with probability 1) that the rain-retrieval problem has a continuum of substantially different solutions – we have no mechanism for identifying a "correct" answer.

In fact, now that we can write down all the deterministic ambiguous profiles giving rise to the same data, it would be interesting to describe the likelihood of occurence of each one, given some reasonable assumptions about the physics governing the problem. With these concerns in mind, let us try to restate the problem in stochastic terms in order to introduce a "measure" on the set of all ambiguous profiles giving rise to the same effective reflectivity profile, and try to find the "average" of this set, along with some measure of the average difference between its members.

3 A minimum-variance algorithm

Let us begin by formulating the problem mathematically. First, we specify all the variables that enter into the problem, and all the hypotheses that we are making about them. Namely, we are trying to estimate the rain rate $R(r)$ as a function of range r. According to our first simple model (1), along with this first variable $R(r)$, we have four others: a, b, α and β. What a priori assumptions can we make about these variables ? Regarding the continuous variable R, we will eventually want to estimate the rain rate at specific discrete ranges. Nevertheless, we should avoid discretizing the range interval until we actually implement our eventual algorithm. The reason is simple: once the unknown function R of the continuous variable r is replaced by discrete unknowns R_i (representing the values of R at sampled range points $i \cdot \Delta r$), it becomes very difficult to put back into the problem the chronological order relating R_i and R_{i+1} and any continuity assumption about R. Instead of discretizing R at the outset, and resorting to an ad hoc artifice to force each R_{i+1} to be "reasonably" close to R_i, we shall build into the problem the assumption that R is a *continuous* function of range. In fact, for simplicity, let us **assume that $R(r)$ is a piecewise linear function of r.** This means that **the slope $s(r)$ of $R(r)$ is piecewise constant.** We would be hard pressed to specify a priori what values s must take, or, indeed, over what range intervals it should remain constant and at what range points it can change values. This is the first source of stochastic behavior in our problem. We will try to make more mathematically rigorous assumptions about it below. **As to the remaining variables a, b, α and β, according to the model (1), we shall assume that each of them has a constant, albeit unknown, value.**

Second, we need to specify the data that we have at our disposal, along with the relation between the data and our variables. According to the model (1), the data will consist of the backscattered power along the radar path. Specifically, let us use the logarithm $y(r)$ of the backscattered power:

$$\begin{aligned} y(r) &= \log(C(r) \cdot p(r)) \text{ with } p(r) \text{ as in equation (1),} \\ &= \log(C(r)) + \log(a) + b \log(R(r)) - 0.2 \log(10)\, \alpha \int_0^r R(t)^\beta dt + \sigma N(r), \end{aligned} \quad (6)$$

where $\log(C(r))$ represents the calibration constant which we assume to be known as before. The quantity $N(r)$ represents a noise term affecting our data, with σ the r.m.s. noise level. We have chosen to pool into the single additive term N all the sources of error that contribute multiplicatively to the received power p. These include mainly Rayleigh fading effect due to the fact that the backscattered cross-section is due to a multitude of scatterers whose distribution within each range volume is unknown and whose echoes have unknown relative phases. This is the second source of stochastic behavior in our problem. To be complete, we should include the effects of system noise, which contributes additively to the measured

power p. We should also make a more mathematically rigorous assumption about the law governing N. We will try to do that below.

Now that we have identified our variables, the a priori constraints on them, and the relation between our data and our variables, we are ready to state the problem: namely, **given these (deterministic and stochastic) constraints and given a particular set of (noisy) data, we would like to obtain the optimal unbiased minimum-variance estimate of our variables.** That is, given some particular data, we want to derive an estimate of $R(r)$ which makes the best use of the information at hand, by being on average (i.e. in the r.m.s. sense) closest to the mean of all the rain profiles that obey the specified constraints and that can be considered possible fits for the data at hand. Writing $X(r)$ for the vector consisting of all our variables at range r, equation (6) can be rewritten as $y(r) = f(X(r)) + \sigma \cdot N(r)$, and our problem can be solved if we can derive an algorithm to obtain the conditional expectation of $X(r)$ given all the measurements $y(r)$.

This estimation problem bears a definite resemblance to the typical problem solved by the Kalman-Bucy filter (see for example [8]). Indeed, in both cases we are given a set of observations at a sequence of times (the sequence of increasing ranges in the case of the radar data). Then, knowing how these observations are affected by the variables which we are trying to estimate (i.e. knowing the formula (6) relating the measured data to the values of our parameters), and knowing the constraints that must be obeyed by the variables themselves, we want to design an algorithm that will estimate as best can be the value of our variables at every point in time (i.e., in our case, range), especially the value of the rain rate itself. The algorithm can (and indeed should) make use of all past information in order to refine at each range step its best estimate for the new value of the rain rate. Thus, this "filtering" would be expected to make up for the inevitable shortcomings of any attempted noise-reduction procedure applied to each individual piece of range-compressed data. The Kalman filter is just such an algorithm, except that it applies only to the linear case, where the effect of the variables on the data is a linear function of the variables. In the problem at hand, that is of course not the case: as is evident in equation (6) the mathematical function f expressing the relation between the data and our variables is far from linear. Fortunately, a generalization of sorts of the Kalman filter to the non-linear case does already exist. Indeed, one can write down the equation that must be solved in order to obtain the "optimal" filter (in the same least-squares sense as the Kalman case) which, when fed a set of not-necessarily-linear observations, will produce the best estimate of the required variables. The equation in question is the Zakai equation, a second-order stochastic partial differential equation whose solution is the conditional density function for our variables, conditioned on the data (a summary is provided for completeness in the appendix – for more details, see [7], [8], [10], [14]). This result has so far not been widely applied because Zakai's equation is, in typical cases, quite difficult if not impossible to solve, exactly or numerically.

Fortunately, in the case at hand, it turns out that it is in fact possible to solve the corresponding equation for the conditional density function, once we have made some simple assumptions about the stochastic behavior of the rain-rate slope variable s, and of the noise term N in the observations. Specifically, we constrain the slope s of the rain rate to be piecewise constant, as before, with slope changes occuring at a mean frequency of λ changes per unit range, and with the new slope s related to the previous slope s' at every slope change in such a way that the difference $s - s'$ is, for simplicity, 0-mean Gaussian with a specified variance σ_s^2. As long as λ and σ_s are strictly positive, this assumption about the rain rate profile simplifies the problem without losing any generality: indeed, *any* continuous function $R(r)$ can be approximated arbitrarily closely by a rain rate profile satisfying our simple constraints. As to N, we shall simply assume that it is a standard normal. This is justifiable by noticing that, if our data consists of the averaged power due to M independent pulses, N would be the average of the squared-magnitudes of M independent standard complex Gaussian variables. Hence, as soon as $M > 4$, it is quite reasonable to assume that N is itself approximately a standard normal variable, and that $\sigma^2 \simeq 1/M$. Under these assumptions, and after introducing an additional variable $c(r) = \int_0^r \alpha R(t)^\beta dt$ representing the accumulated attenuation up to range r, one can indeed write down the Zakai differential equation governing the evolution with r of the conditional density function $\mathcal{P}|_r(c, R, s, a, b, \alpha, \beta)$ at range r, conditioned on the data $\{y(t),\ t \leq r\}$, and, in fact, solve it exactly. Indeed, in the appendix, we show how, starting with $\mathcal{P}|_{r=r_0}(c, R, s, a, b, \alpha, \beta)$ at any range r_0, one can account for all the data $y(r)$ with $r_0 < r < r_1$ to calculate the density function $\mathcal{P}|_{r=r_1}(c, R, s, a, b, \alpha, \beta)$ at any range $r_1 > r_0$.

Armed with this algorithm, our strategy is as follows:

- Start with an a priori density function $\mathcal{P}|_{r=0}(c, R, s, a, b, \alpha, \beta)$ which, for lack of any more precise knowledge, is uniform in R (resp. a, b, α, β) over a pre-determined range $[R_{\min}, R_{\max}]$ (resp. $[a_{\min}, a_{\max}]$, $[b_{\min}, b_{\max}]$, $[\alpha_{\min}, \alpha_{\max}]$, $[\beta_{\min}, \beta_{\max}]$),
- update $\mathcal{P}|_r$ by using our algorithm to incorporate each new piece of data with increasing range r, from $r = 0$ down to $r = r_s =$ the range of the surface, at which time $\mathcal{P}|_{r_s}$ would be the density function for $R(r_s)$ conditioned on *all* the data,
- update $\mathcal{P}|_r$ backwards by starting with $\mathcal{P}|_{r_s}$ as the initial density function, running r backward, and using our algorithm to obtain $\mathcal{P}|_r$ at all $r < r_s$.

Once the conditional densities $\mathcal{P}|_r$ have been computed at every range point r, the conditional mean

$$\hat{R}(r) = \int\int\int\int\int\int\int R\,\mathcal{P}|_r(c, R, s, a, b, \alpha, \beta)\, dc\, dR\, ds\, da\, db\, d\alpha\, d\beta \tag{7}$$

gives the estimate of the rain rate at range r, and the conditional variance

$$\hat{v}(r) = \int\int\int\int\int\int\int (R - \hat{R}(r))^2\, \mathcal{P}|_r(c, R, s, a, b, \alpha, \beta)\, dc\, dR\, ds\, da\, db\, d\alpha\, d\beta \tag{8}$$

is the corresponding estimate of the variance of the rain rate at range r.

Before going on to the applications, note that the algorithm that we propose requires a larger amount of computation than the corresponding "extended" Kalman filter would require. Indeed, there are several ways to extend the linear Kalman filtering procedure to non-linear problems such as the on ewe have, by making appropriate linearizing approximations. The resulting extended Kalman filter would produce an algorithm wihch calculates the moments $\hat{R}(r)$ and $\hat{v}(r)$ directly (along with the means and covariances of all our remaining variables c, s, a, b, α and β), without having to calculate the full density function $\mathcal{P}$ of the variables at every range step. While the extended Kalman filter approach would produce a fast-running computer code, the full Zakai-equation approach gives us one significant advantage: namely, the conditional density function that it computes can be used as a new a priori probability density function for the rain parameters, accounting only for the radar measurements. Any additional data can then be used to refine the estimated of these parameters by further conditioning $\mathcal{P}$ on the new data. In addition to obtaining estimates of our parameters that are optimal up to the various approximations made, we can perform the optimal fusion of the radar data with any other data that becomes available, such as radiometer measurement of the brightness temperature at various frequencies.

Before going on to the applications, we also note that the algorithm described above relies on the model given by equations (1) and (6), where the $Z - R$ and $k - R$ relations were assumed to be power laws with constant (if unknown) coefficients. We chose these constant power laws in order to study the approach under the simplest assumptions. The minimum-variance approach itself, however, can be applied with any set of initial hypotheses. Indeed, the equation for the conditional density function in the case where one assumes a range-dependent Γ-drop-size-distribution can be derived in a similar fashion, and its solution would allow one to calculate the rain-rate estimate and its variance for this more realistic model of the relation between the rain and the radar quantities. Preliminary results that we have obtained in this direction are encouraging, and we intend to report on our progress in further publications.

Finally, we assumed in equation (6) that the range-dependent calibration term $\mathcal{C}(r)$ was known exactly at every range r. If this is not the case in practice, the uncertainty in $\mathcal{C}(r)$ can be incorporated into the noise term, by appropriately increasing σ in (6). In fact, additional sources of error, such as additive system noise, can also be incorporated. For example, in the typical case where the system noise voltage is white, the sum of the voltage due to system noise with the voltage due to rain echo will again be Gaussian, and its power will be the sum of the powers of the two summands. In this case, equation (6) would become

$$y(r) = \log\left((\mathcal{C}(r) \cdot p(r)) + \sigma_n^2\right) + \sigma \cdot N \tag{9}$$

with $C(r)$ the known range-dependent calibration constant, σ_n^2 the known constant system noise power, $p(r)$ the formula relating the effective reflectivity to the rain parameters of whatever rain model one wishes to use (formula (1) for example), and $\sigma^2 \simeq$ the inverse of the number of effective independent pulses averaged in each look.

4 Applications

In this section, we apply the approach developed in the previous section to some typical examples. In each case, we will be interested in processing effective reflectivities at discrete ranges, and obtaining rain rate estimates at discrete ranges. While the exact mathematical details are given in the appendix for the continuous case, discretized versions of $\mathcal{P}$ and of the equation governing its evolution are not difficult to write down. For our purposes, we shall use the following approximate discretization of the formula for $\mathcal{P}$ given in the appendix:

$$\mathcal{P}'_{r+\delta}(c,R,s,a,b,\alpha,\beta) = \left(\mathcal{P}_r(c',R',s,a,b,\alpha,\beta) + \lambda \sum_{s'} \mathcal{P}_r(c',R',s',a,b,\alpha,\beta) g(s-s')\right) \cdot e^{-H} \tag{10}$$

which tells us how to compute the unnormalized version $\mathcal{P}'$ of $\mathcal{P}$ at range $r+\delta$, given $\mathcal{P}$ at range r, and given the logarithm $y(r+\delta)$ of the received power, averaged over M pulses. In equation (10), we used the abbreviations H, c', R' for

$$\begin{aligned} H &= \frac{1}{2\sigma^2}\left(\log(C(r)aR^b 10^{-0.2c} + \sigma_n^2) - y(r+\delta)\right)^2, \\ g(x) &= \frac{e^{-x^2/2\sigma_s^2}}{\sqrt{2\pi\sigma_s^2}}, \\ c' &= c - \alpha(R - s\delta/2)^\beta \delta, \\ R' &= R - s\delta. \end{aligned}$$

The normalized density function $\mathcal{P}_{r+\delta}$ is obtained by dividing $\mathcal{P}'_{r+\delta}$ by the normalizing constant $\sum_c \sum_R \sum_s \sum_a \sum_b \sum_\alpha \sum_\beta \mathcal{P}'_{r+\delta}(c,R,s,a,b,\alpha,\beta)$. The parameters which the user must specify as input to the algorithm are the calibration function $C(r)$, the system noise power σ_n^2, the number M of effectively independent pulses averaged in one look (so that we may set $\sigma^2 = 1/M$), the average frequency λ of the rain-rate slope changes, and the r.m.s. value σ_s of the slope difference $s_{\text{new}} - s_{\text{old}}$ when a slope change does occur. Formula (10) itself is relatively easy to implement numerically. It clearly shows that the algorithm proceeds at every new range in two steps: first, it smoothes $\mathcal{P}$ in order to account for the possible changes in the local slope of R, then it multiplies the resulting smoothed function by weights

that are largest for those values of the parameters that best fit the received data. It is interesting to note that this two-step process is very similar to other proposed methods for approximating the solution to the general nonlinear filtering problem ([7]). Let us now look at specific examples.

Our first application is the serendipitous observation that if we force the a priori unknown constants a, b, α, β to take on know values $a_0, b_0, \alpha_0, \beta_0$, i.e. if we set the interval bounds $a_{\min} = a_{\max} = a_0$, $b_{\min} = b_{\max} = b_0$, $\alpha_{\min} = \alpha_{\max} = \alpha_0$, $\beta_{\min} = \beta_{\max} = \beta_0$, our algorithm becomes in effect a numerically stable Hitschfeld-Bordan rain-rate retrieval algorithm! As an illustration, we considered the reflectivity profile that would be produced by the constant rain rate $R_0 = 20$ mm/hr over the range $0 \leq r \leq 3$ km, as in the examples in section 2, this time with $a_0 = 300$, $b_0 = 1.5$, $\alpha_0 = 0.026$, $\beta_0 = 1.08$. We synthesized the effective reflectivity as it would be measured every $\delta = 0.05$ km, asuming that $M = 50$ pulses are averaged so that $\sigma = 1/\sqrt{50} \simeq 0.14$. We assumed that the calibration constant was known exactly, that there was no system noise, and that the only remaining inputs to the retrieval problem, aside from the synthesized data, were the initial density function $\mathcal{P}|_{r=0}(c, R, s)$ and the rain-rate constraint parameters λ and σ_s. We started with $\mathcal{P}_{r=0}$ uniform in R over the range $0 < R \leq 50$ mm/hr, uniform in s over the range $-40 < s < 40$ (mm/hr)/km, and a δ-function in c (since the accumulated attenuation at range 0 is always 0 with probability 1). As to the remaining two parameters, we decided to vary their settings over a range of realistic values, namely $1/2 \leq \lambda\delta < 20$ and $1 \leq \sigma_s\delta \leq 10$. Heuristically, the value $\lambda = 0.5/\delta$ implies that we know a priori that the (piecewise constant) slope of the rain rate profile can change once every 2δ units of range on average, allowing for slow changes only, while the value $\lambda = 20/\delta$ implies that slope of the rain rate profile changes about 20 times between two consecutive measurements, which allows for many readjustments in the slope. While the parameter λ constrains the *frequency* of the allowable variations in the profile as a function of range, the parameter σ_s restricts the *amount* of variation when it does occur. The value $\sigma_s = 1/\delta$ implies that the allowable change in slope has an r.m.s. value of 1 mm/hr per $\delta = 50$ m of range, while the value $\sigma_s = 10/\delta$ implies that the r.m.s. change in slope is 10 mm/hr per 50 m of range. In practice, one should keep in mind that our discrete sampling strategy forces σ_s to remain between the original bounds $1 \leq \sigma_s\delta \leq 10$.

Figure 3 shows the two estimated rain rate profiles $\hat{R}_i(r)$ $(i = 1, 2)$ that were obtained by our algorithm using the inputs above with $\lambda\delta = 5$ and $\sigma_s\delta = 10$ for $i = 1$, and $\lambda\delta = 20$ and $\sigma_s\delta = 2$ for $i = 2$. The error bars are the values of the square root of the estimate of the conditional variance $\hat{v}_1(r)$ for the case $i = 1$. These graphs are typical of the profiles we obtained by varying λ and σ_s over the range of values given above. The variance was smallest when when we gave λ and σ_s the smallest values in their respective ranges, and they were largest when λ and σ_s were largest. The smallest value we obtained for $\sqrt{\hat{v}(r)}$ was 0.55, the largest 1.6 mm/hr. The bias in the estimate $\hat{R}(r)$ itself never exceeded 1

mm/hr. While this bias is due to the approximations and the discretization, the variance is the true variance of the estimate. Yet we have assumed that the rain parameters a, b, α and β were known exactly in this case. They cannot be the source of the uncertainty. The only remaining source of ambiguity is the noise in the data. Let us examine this noise term in more detail. Since the rain rate is constant in this case, equation (6) shows that the two terms that vary in the measurements from one range point to the next are the noise term σN and the incremental attenuation $\simeq 0.2\log(10)\alpha R_0^\beta \delta$, which is approximately $(0.2)\cdot(2.3)\cdot(0.026)\cdot(25.4)\cdot(0.05)$, or about 0.0152. Compared to $\sigma \simeq 0.14$, this is a very small quantity indeed to try to estimate exactly. The variance estimated by our algorithm is a direct result of this discrepancy between the size of the incremental attenuation and the noise in the measurements. It is therefore natural that this variance is reduced when we tighten our constraints (by appropriately decreasing the values of λ and σ_s) to in effect help the algorithm by telling it that the profile is almost surely constant.

While the case of a constant rain rate profile is a good example because of its simplicity, it is not very realistic. Indeed, no real data will show a spontaneous jump in the measured reflectivity, from no data to the kinds of numbers associated with 20 mm/hr of constant rain. Keeping all the other parameters exactly as above, we considered three different, somewhat more realistic, rain rate profiles by synthesizing the effective reflectivity profiles that they would produce: case A where the rain rate increases linearly from 3 to 21 mm/hr; case B where the rain rate increases linearly from 3 mm/hr at range $r = 0$ to 21.5 mm/hr at $r = 1.5$ km, then decreases linearly to 6.5 mm/hr at $r = 3$ km; and a saw-tooth case C, where the rain rate increases linearly from 3 mm/hr at range $r = 0$ to 30 mm/hr at $r = 1.2$ km, rapidly decreases linearly back to 3 mm/hr at $r = 1.5$ km, and repeats the pattern to $r = 3$ km. Figure 4 (resp. 5) shows the estimated rain rate profiles $\hat{R}_i(r)$ $(i = 1, 2)$ using our algorithm with the input above and $\lambda\delta = 5$ and $\sigma_s\delta = 10$ for $i = 1$, and $\lambda\delta = 20$ and $\sigma_s\delta = 2$ for $i = 2$ for case A (resp. case B). As before, the error bars are the values of the square root of the estimate of the conditional variance $\hat{v}_1(r)$ for the case $i = 1$. Figure 6 shows the exact saw-tooth profile of case C, and the estimated rain rate profile for $\lambda\delta = 5$ and $\sigma_s\delta = 2$, along with the corresponding estimate of the standard deviation. It is interesting to note that while the estimate seems quite good on the up-slopes, it is consistently below the true value on the down-slopes. This is due to the a priori constraint on our variable s: indeed, the assumption $-40 < s < 40$ mm/hr per km limits the allowable rain rate profiles to changes of no more than 12 mm/hr over 300 m - but on the 300m-down-slope of our saw-tooth profile the rain rate decreases by 27 mm/hr ! Once we expand the range of s appropriately, our algorithm produces an estimate that is much closer to the true rain rate, as the previous examples would lead us to expect. This is evident in figure 7, where we plot the rain rate profile estimated by our algorithm with the same inputs as before, except that s is now allowed to range over the interval $[-100, 100]$ mm/hr/km.

Let us now examine what happens when we allow the variables a, b and α to be unknown. We selected the reflectivity profile of case B, the more realistic of the four cases that we considered above. While the reflectivities were synthesized using the values $a = 300$, $b = 1.5$ and $\alpha = 0.026$, the algorithm was told only that a was in the interval $[200, 400]$, b was in the interval $[1.4, 1.6]$, and that α was in the interval $[0.018, 0.034]$. We started with $\mathcal{P}_{r=0}$ uniform in R over the range $0 < R \leq 50$ mm/hr, uniform in s over the range $-40 < s < 40$ (mm/hr)/km, and a δ-function in c as before. For λ and σ_s, we decided to use values in the middle of the ranges considered in the previous examples, namely $\lambda\delta = 5$ and $\sigma_s\delta = 2$ mm/hr (with $\delta = 50$ meters). Figure 8 shows the rain rate profile estimated by our algorithm, along with the estimated r.m.s. uncertainty $\sqrt{\hat{v}(r)}$. One might notice that the ambiguity seems to increase almost linearly with the rain rate values. In fact, the relative r.m.s. uncertainty $\sqrt{\hat{v}(r)}/\hat{R}(r)$ varies between 20 and 36 % in this case. The two curves framing our estimate are the rain rates that give the same echo profile when $\alpha = 0.034$ (top curve), and when $\alpha = 0.018$ (bottom curve). While the estimated rain rate profile itself does lie between these two extreme curves, it appears to be significantly larger than the original rain rate (see figure 5). As was pointed out earlier, comparison with the original rain rate profile is not a true measure of the effectiveness of the algorithm. Rather, we must check that the estimated reflectivities are close to the actual reflectivity profile. Figure 9 shows the dBZ values for the synthesized profile as well as for the echo profile estimated by our algorithm. It is reassuring to note that the estimated echo profile does remain within 0.3 dBZ of the actual echo profile. This implies that the echo profile produced by our estimated rain values is within $\pm$ 7 % of the actual (synthesized) echo at all ranges.

The next four figures illustrate the effects of changing the constraints on our state variables. Figure 10 shows the estimated profile and r.m.s. uncertainty when the constraint on the variable α is changed to $0.026 \leq \alpha \leq 0.034$. The estimate is higher than the previous one because increasing the attenuation rate allows the rain rates to increase without changing the echo power. The relative uncertainty in this case varies between 18 and 39 %. These values are comparable to the ones obtained in the previous case, in spite of the fact that the interval over which α is now allowed to range has shrunk by 100 %. This seems to imply that the *relative* r.m.s. error does increase when the rain rate values increase. The next case confirms this trend. Figure 11 shows the estimated profile and r.m.s. uncertainty when the constraint on the variable α is $0.01 \leq \alpha \leq 0.026$. The estimate is below the previous ones, reflecting the fact that a decrease in the attenuation rate implies a corresponding decrease in the rain rates that can produce a given echo power. The relative uncertainty in this case varies between 19 and 30 %, a range somewhat smaller than the one that was obtained under the assumption $0.018 \leq \alpha \leq 0.034$, although the intervals for α in these two cases have the same width. The plots of the echo profile corresponding to figures 10 and 11 are indistinguishable from the one of figure 9. Finally, figure 12 shows the estimated profile and

r.m.s. uncertainty when the initial constraint on the rain rate variable R itself is changed to $0 < R < 25$, keeping α in the original range $[0.018, 0.034]$. The corresponding drop in the estimated rain rate profile is accompanied by a decrease in the r.m.s. uncertainty to values between 17 and 27 %. Figure 13 shows the estimated echo profile for this case: it is quite similar to the one of figure 9, except that the difference between the estimates and the actual echo never exceeds 0.27 dBZ in this case. This implies that the echo profile produced by our estimated rain values in this case remains within $\pm$ 6 % of the actual effective reflectivity profile.

5 Acknowledgements

This work was performed at the Jet Propulsion Laboratory, California Institute of Technology, in support of the Tropical Rainfall Measuring Mission, under contract with the National Aeronautics and Space Administration.

References

[1] D. Atlas and C.W. Ulbrich: *Path and area-integrated rainfall measurement by microwave attenuation in the 1-3 cm band*, J. Appl. Meteor. 16, 1977, pp. 1322-1331.

[2] R.J. Doviak and D.S. Zrnić: *Doppler radar and weather observations*, Academic Press, 1984.

[3] Duc Kong Kieu: *Radar rainfall measurements from space*, Ph.D. dissertation, Kansas University, 1991.

[4] Fujita M.: *An algorithm for estimating rain rate by a dual-frequency radar*, Radio science 18, 1983, pp. 697-708.

[5] W. Hitschfeld and J. Bordan: *Errors inherent in the radar measurement of rainfall at attenuating wavelengths*, J. Meteor. 11, 1954, pp. 58-67.

[6] Z.S. Haddad, E. Im and S. Durden: *Ambiguities in the estimation of rain rates from radar returns at attenuationg wavelengths*, preprint.

[7] W.E. Hopkins and W.S. Wong: *Lie-Trotter product formulas for nonlinear filtering*, Stochastics 17, 1985, pp. 313-337.

[8] A. Jazwinski: *Stochastic processes and filtering theory*, Academic Press, 1970.

[9] Kozu T. and Nakamura K.: *Rainfall parameter estimation from dual-radar measurements combining reflectivity profile and path-integrated attenuation*, J. Atmos. Oceanic Technol. 8, 1991, pp. 259-270.

[10] R.S. Lipster and A.N. Shiryayev: *Statistics of random processes*, Springer Verlag, 1977.

[11] M. Marzoug and P. Amayenc: *Improved range-profiling algorithm of rainfall rate from a spaceborne radar with path-integrated attenuation constraint* , I.E.E.E. Trans. Geosci. Rem. Sens. 29, 1991, pp. 584-592.

[12] R. Meneghini and Kozu T.: *Spaceborne weather radar*, Artech House, 1990.

[13] C.W. Ulbrich: *Natural variations in the analytical form of the raindrop size distribution*, J. Clim. Appl. Meteo. 22, 1983, pp. 1764-1775.

[14] M. Zakai: *On the optimal filtering of diffusion processes*, Z. Wahrsch. verw. Geb. 11, 1969, pp. 230-243.

A Appendix: the Zakai equation

Here is a simplified summary of those results of non-linear filtering which we will need. For a complete account, see for example [7], [8], [10], [14]. Assume that $X(t)$ is a stochastic process in $\mathbf{R}^n$ satisfying the stochastic equation

$$dX(t) = h(X(t))dt + g(X(t))dB(t) \tag{11}$$

where $h : \mathbf{R}^n \longrightarrow \mathbf{R}^n$ and $g : \mathbf{R}^n \longrightarrow \{n \times m \text{ matrices}\}$ are twice-differentiable functions, and $B(t)$ is standard Brownian motion in $\mathbf{R}^m$. Assume we have observations $Y(t)$ (a stochastic process in $\mathbf{R}$) which obey

$$dY(t) = f(X(t))dt + \sigma db(t) \tag{12}$$

where σ is a real constant, $f : \mathbf{R}^n \longrightarrow \mathbf{R}$ is a differentiable function, and $b(t)$ is standard Brownian motion in $\mathbf{R}$. Assume further that $B(t)$, $b(t')$ and $X(0)$ are independent for all t different from t'. Given an initial density ρ_0 for the states of $X(0)$, the conditional density $\rho(t, x \mid Y(s)\, s \leq t)$ for $X(t)$, given all $Y(s)$ up to time t, must satisfy the (Zakai) equation

$$\frac{\partial \tilde{\rho}}{\partial t} = D\tilde{\rho} - \frac{1}{\sigma^2} Y(t) \cdot D'\tilde{\rho} + \frac{1}{\sigma^2} \left(Y(t) \cdot D''Y(t)\right) \tilde{\rho} \tag{13}$$

where ρ and $\tilde{\rho}$ are related by $\rho(t, x) = K(t) e^{Y(t) \cdot f(x)/\sigma^2} \tilde{\rho}(t, x)$ in which the function K takes that value making $\int \rho(t, x) dx = 1$ for all t, and where the operator D is given by

$$D\tilde{\rho} = \frac{1}{2} \sum_{i,j} \frac{\partial^2}{\partial x_i \partial x_j} \left((gg^T)_{ij} \tilde{\rho} \right) - h \cdot \nabla \tilde{\rho} - (\mathrm{div}(h))\tilde{\rho} - \frac{1}{2\sigma^2} |f|^2 \tilde{\rho} \tag{14}$$

(here g^T denotes the transpose of the matrix g, and $\mathrm{div}(h)$ denotes the divergence of h), the operator D' is given by

$$D'\ \tilde{\rho} = [f, D]\tilde{\rho} \tag{15}$$

(where the term on the right refers to the commutator of the two operators "multiplication by f" and D), and the operator D'' is given by

$$D''\tilde{\rho} = \frac{1}{2}[f, [f, D]]\tilde{\rho} \tag{16}$$

Once ρ has been computed by solving the Zakai equation with initial condition $\rho|_{t=0} = \rho_0$, the required conditional expectation $\mathcal{E}\{X(t) \mid Y(\tau), 0 \leq \tau \leq t\}$ can be computed by performing the integral $\mathcal{E}\{X(t) \mid Y(\tau), 0 \leq \tau \leq t\} = \int x\rho(t, x) dx$. Note that if f, g and h are linear, i.e. when the filtering problem is linear, Kalman showed that the conditional expectation can then be calculated directly by solving a coupled system consisting of a linear equation in n variables driven by the observations, coupled to a Riccati equation in $n(n+1)/2$ variables involving the second moment only. That is infinitely more manageable than having to find the function ρ of $n+1$ variables solving the Zakai partial differential equation.

B Appendix: Solving the Zakai equation

In our case, the "time" variable is actually the range r. Moreover, $X(r)$ is the vector $(c(r), R(r), s(r), a, b, \alpha, \beta)$, with the constraints that $dc = \alpha R^\beta dr$, $dR = s\,dr$, that a, b, α and β are constant, and that the slope $s(r)$ is a jump process taking independent values, with density g, which are constant between the jumps of a Poisson process of rate λ. Heuristically, this means that the graphs of the rain rates that we consider are broken line segments, with slope changes at a sequence of ranges $\{r_1, r_2, r_3, ...\}$ such that the segment lengths $r_1, r_2 - r_1, r_3 - r_2$, ..., are distributed according to a Poisson distribution of mean $1/\lambda$, and such that the new slopes at each "break" are distributed according to a prespecified density function g. The introduction of $c(r)$ as an additional state variable is technically necessary in order for the stochastic process $X(r)$ to be Markov. Finally, writing $Y(r) = \int_0^r y(r')\,dr'$, with y as in equation (6) of section 3, we assume that

$$dY(r) = f(X(r))dr + \sigma db(r) \tag{17}$$

where "db/dr" would be the white noise process, and where

$$f(c, R, s, a, b, \alpha, \beta) = \log(\mathcal{C}(r) \cdot aR^b \cdot 10^{-0.2c} + \sigma_n^2) \tag{18}$$

with $\mathcal{C}(r)$ the known calibration constant, and with σ_n (resp. σ) the known additive system noise (resp. multiplicative fading noise) variance.

Under these assumptions, the Zakai differential equation (13) governing the evolution with r of the unnormalized conditional density function $\tilde{\mathcal{P}}_r(c, R, s, a, b, \alpha, \beta)$ conditioned on the data $\{y(r'),\ r' \le r\}$ is

$$\frac{\partial \tilde{\mathcal{P}}}{\partial r} = -\alpha R^\beta \frac{\partial \tilde{\mathcal{P}}}{\partial c} - s\frac{\partial \tilde{\mathcal{P}}}{\partial R} - \frac{1}{2\sigma^2} F_r(c, R, s, a, b, \alpha, \beta)\tilde{\mathcal{P}} + \lambda \int \tilde{\mathcal{P}}(c, R, s', a, b, \alpha, \beta) g(s - s')ds' \tag{19}$$

where the function $F(r, c, R, s, a, b, \alpha, \beta)$ is given by

$$F = f^2 + 2(\alpha R^\beta \frac{\partial f}{\partial c} + s\frac{\partial f}{\partial R})Y(r) + \lambda. \tag{20}$$

A natural attempt to solve this equation is to use the "cascade" approach. Specifically, we write $\tilde{\mathcal{P}} = \sum_{n \ge 0} \tilde{\mathcal{P}}^{(n)}$, and require that each $\tilde{\mathcal{P}}^{(n)}$ satisfy

$$\frac{\partial \tilde{\mathcal{P}}^{(n)}}{\partial r} = -\alpha R^\beta \frac{\partial \tilde{\mathcal{P}}^{(n)}}{\partial c} - s\frac{\partial \tilde{\mathcal{P}}^{(n)}}{\partial R} - \frac{1}{2\sigma^2} F \cdot \tilde{\mathcal{P}}^{(n)} + \lambda \int \tilde{\mathcal{P}}^{(n-1)}(c, R, s', a, b, \alpha, \beta) g(s - s')ds' \tag{21}$$

where $\hat{\mathcal{P}}^{(-1)}$ is assumed to be identically zero. This is justified because the requirement that $\hat{\mathcal{P}}$ satisfy equation (19) is exactly equivalent to the requirement that each $\hat{\mathcal{P}}^{(n)}$ satisfy equation (21).

The introduction of the index n makes it possible to solve our problem exactly. Indeed, the system of inhomogeneous first order equations (21) can be solved by induction, using the method of characteristics. For example, (21) with $n = 0$ is a homogeneous equation with no forcing term (because $\mathcal{P}^{(-1)}$ is identically 0): it can therefore be solved easily using characteristics. In fact, its solution is

$$\hat{\mathcal{P}}_r^{(0)}(c,R,s,a,b,\alpha,\beta) = \mathcal{P}|_{r=0}(c-\alpha\frac{R^{\beta+1}-(R-sr)^{\beta+1}}{s(\beta+1)}, R-sr, s, a, b, \alpha, \beta) \tag{22}$$
$$\cdot \exp\left(-\frac{1}{2\sigma^2}\int_0^r F(r', c-\alpha\frac{R^{\beta+1}-(R-s(r-r'))^{\beta+1}}{s(\beta+1)}, R-s(r-r'), s, a, b, \alpha, \beta)dr'\right)$$

where the initial density $\mathcal{P}|_{r=0}$ is assumed known. Practically, a slightly more general version of this equation, relating $\hat{\mathcal{P}}$ at range r_1 to $\hat{\mathcal{P}}$ at any range $r_0 < r_1$, would be useful. Such an expression can indeed be written down. To keep the formulas relatively uncluttered, we shall use the notation

$$c'(\Delta r) = c-\alpha\frac{R^{\beta+1}-(R-s\Delta r)^{\beta+1}}{s(\beta+1)}, \tag{23}$$
$$R'(\Delta r) = R-s\Delta r. \tag{24}$$

Using this notation, the general solution $\hat{\mathcal{P}}^{(n)}$ to equation (21) for any $n \geq 0$ can be written as

$$\hat{\mathcal{P}}_{r_1}^{(n)}(c,R,s,a,b,\alpha,\beta) = \hat{\mathcal{P}}_{r_0}^{(n)}(c'(r_1-r_0), R'(r_1-r_0), s, a, b, \alpha, \beta)\, e^{-\frac{1}{2\sigma^2}\int_{r_0}^{r_1} F(r', c'(r_1-r'), R'(r_1-r'), s, a, b, \alpha, \beta)dr'}$$
$$+\lambda\int_{r_0}^{r_1}\left(\int \hat{\mathcal{P}}_r^{(n-1)}(c'(r_1-r), R'(r_1-r), s', a, b, \alpha, \beta)g(s-s')ds'\right) e^{-\frac{1}{2\sigma^2}\int_r^{r_1} F(r', c'(r_1-r'), R'(r_1-r'), s, a, b, \alpha, \beta)dr'} dr \tag{25}$$

keeping in mind that $\hat{\mathcal{P}}^{(-1)}$ is zero.

That these formulas for $\hat{\mathcal{P}}^{(n)}$ do give solutions to the prescribed equations (21) for $\hat{\mathcal{P}}^{(n)}$ can be verified directly. One can then reconstitute $\hat{\mathcal{P}}$ itself by adding all these equations together. Remarkably, the equation one then gets is exactly this last equation without the index n ! Indeed, the left-hand-sides add up to $\hat{\mathcal{P}}$ at range r, and the right-hand-sides involve the values of $\hat{\mathcal{P}}$ at earlier ranges. In our case, one can thus compute $\mathcal{P}$ by "recursion" on r, starting with a given $\mathcal{P}|_{r=0}$, applying the formula

$$\hat{\mathcal{P}}_{r_1}(c,R,s,a,b,\alpha,\beta) = \hat{\mathcal{P}}_{r_0}(c'(r_1-r_0),R'(r_1-r_0),s,a,b,\alpha,\beta)\, e^{-\frac{1}{2\sigma^2}\int_{r_0}^{r_1} F(r',c'(r_1-r'),R'(r_1-r'),s,a,b,\alpha,\beta)dr'}$$
$$+\lambda\int_{r_0}^{r_1}\left(\int \hat{\mathcal{P}}_r(c'(r_1-r),R'(r_1-r),s',a,b,\alpha,\beta)g(s-s')ds'\right) e^{-\frac{1}{2\sigma^2}\int_{r}^{r_1} F(r',c'(r_1-r'),R'(r_1-r'),s,a,b,\alpha,\beta)dr'}dr \tag{26}$$

repeatedly, and using the fact that $\mathcal{P}$ and $\hat{\mathcal{P}}$ are related by $\mathcal{P} = Kc^{Y\cdot f/\sigma^2}\hat{\mathcal{P}}$ with K = that scalar that makes $\mathcal{P}$ integrate to 1.

Figure 1: surface-reference curves

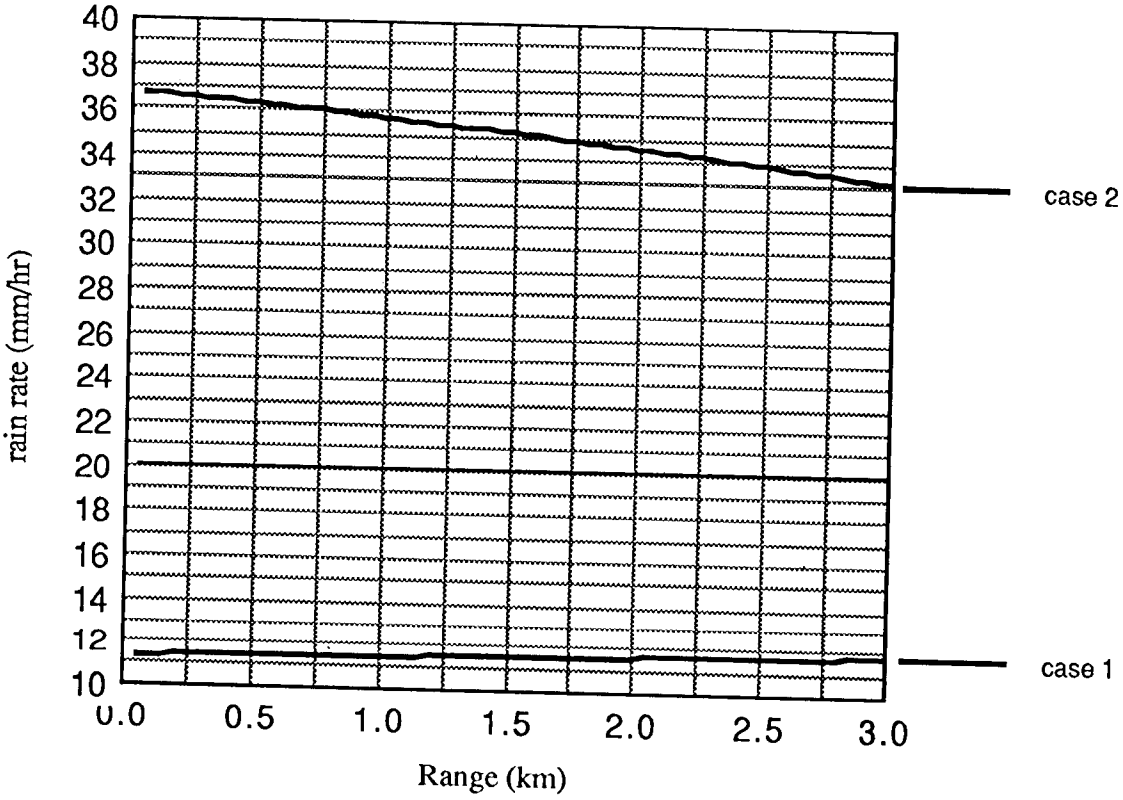

Figure 2: DSD curves

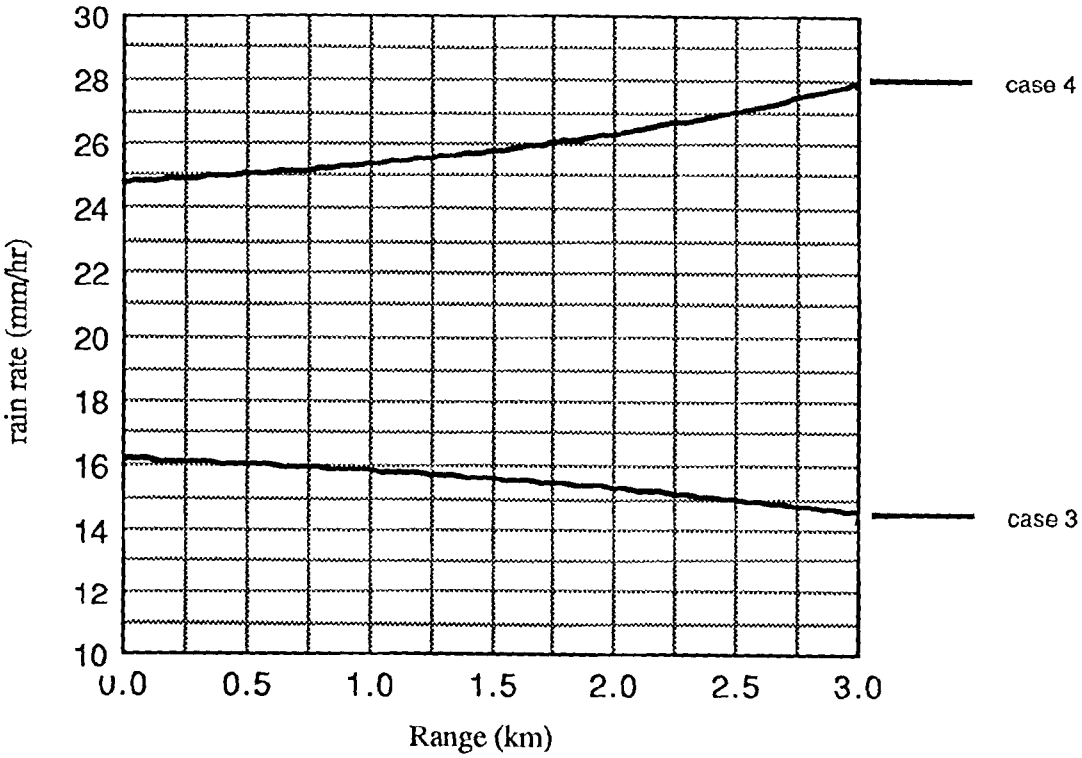

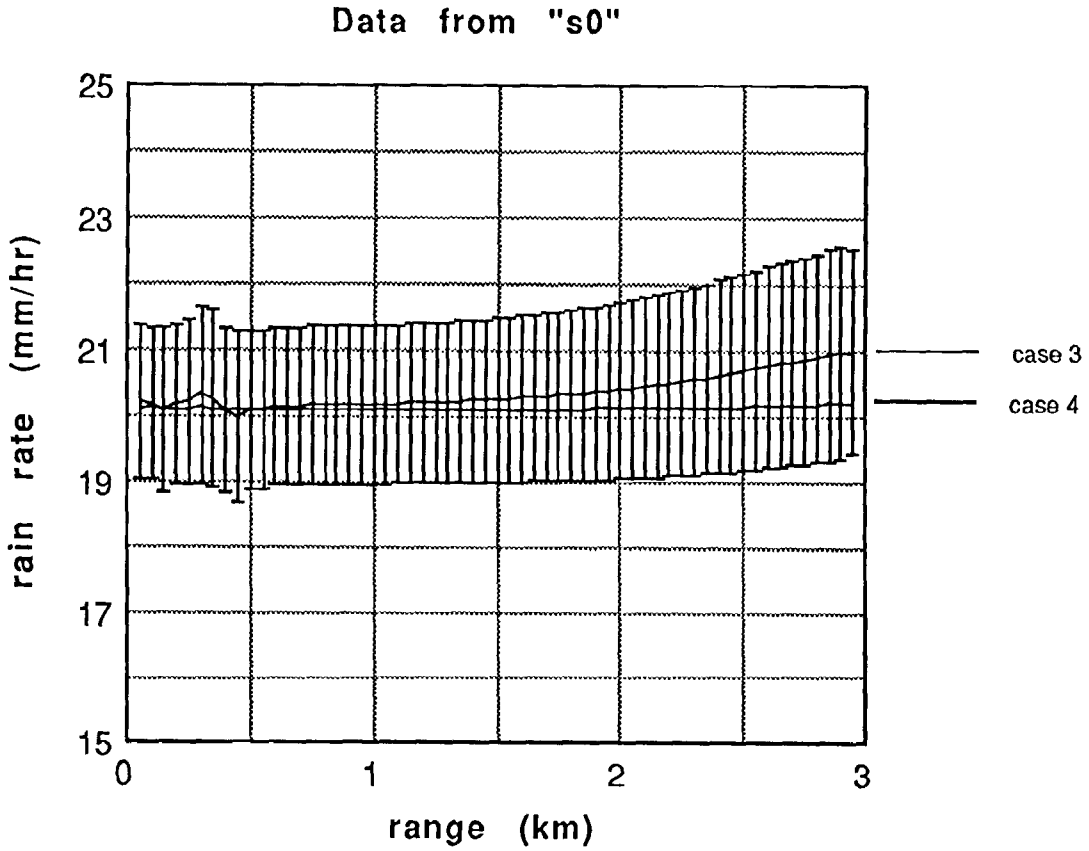
Data from "s0"
25
23
21
19
17
15
rain rate (mm/hr)
0
1
2
3
range (km)
case 3
case 4

Figure 3

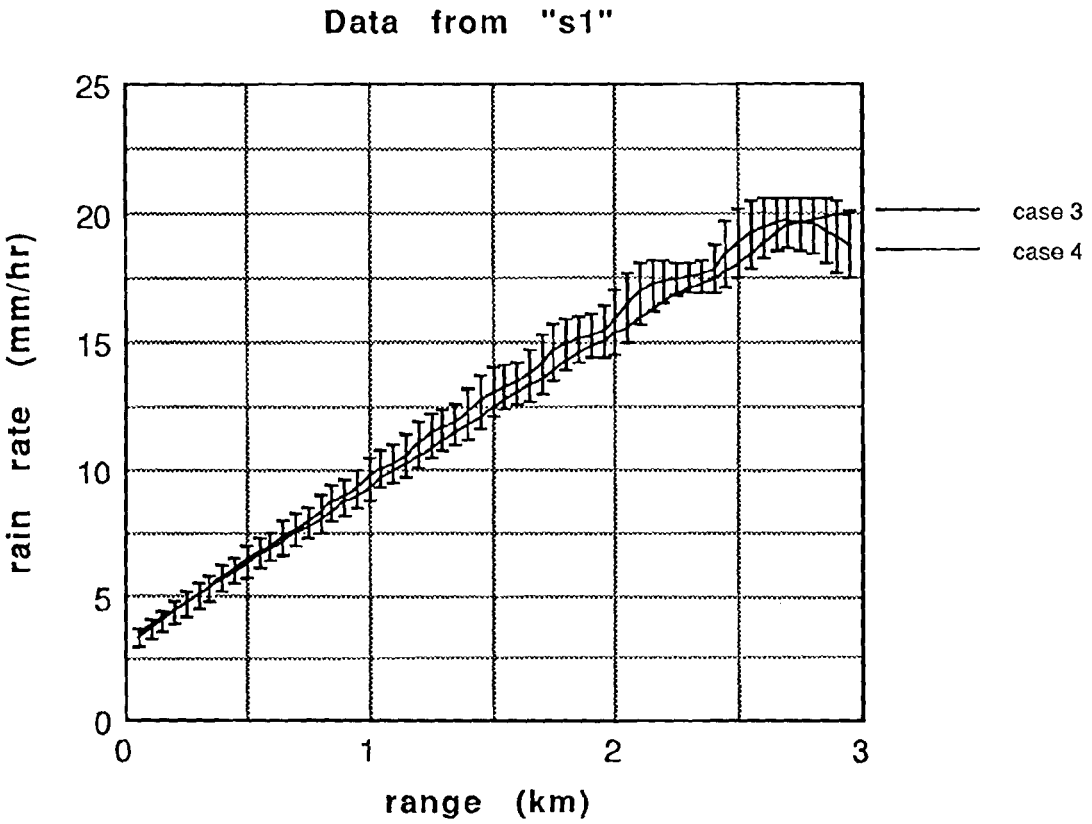
Data from "s1"
rain rate (mm/hr)
25
20
15
10
5
0
0
1
2
3
range (km)
case 3
case 4

Figure 4

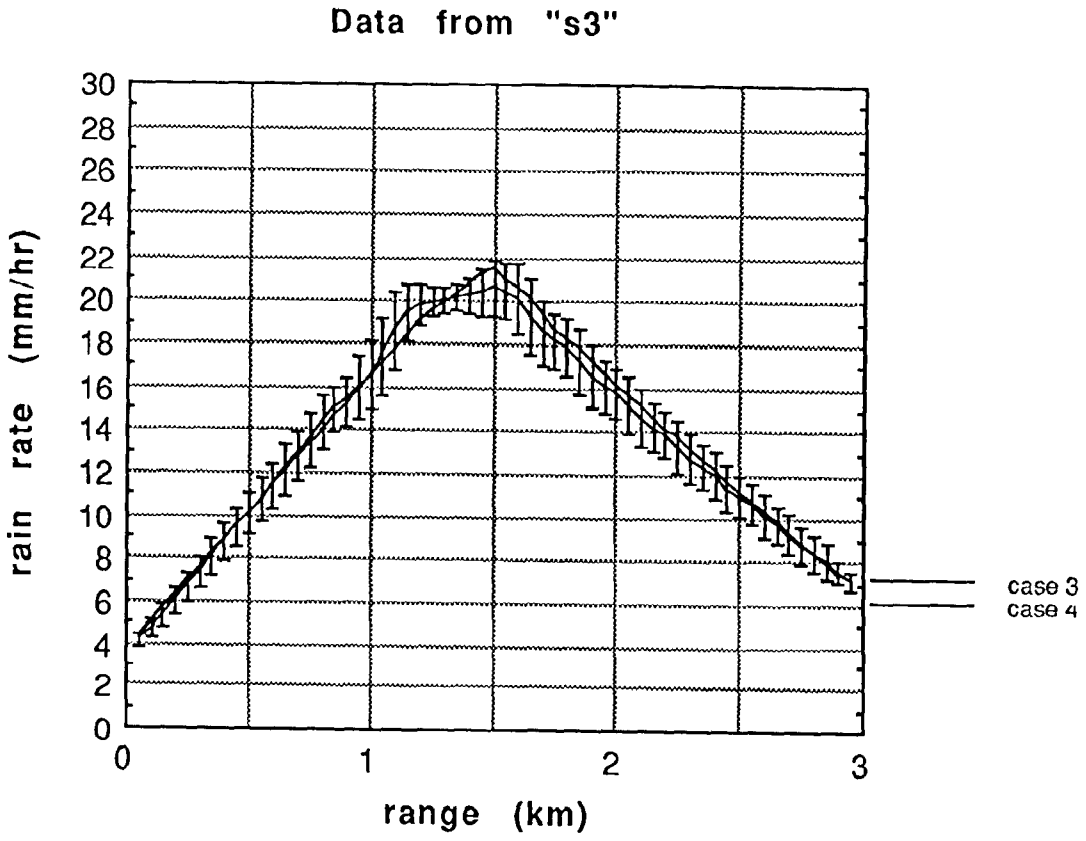
Data from "s3"
rain rate (mm/hr)
30
28
26
24
22
20
18
16
14
12
10
8
6
4
2
0
0
1
2
3
range (km)
case 3
case 4

Figure 5

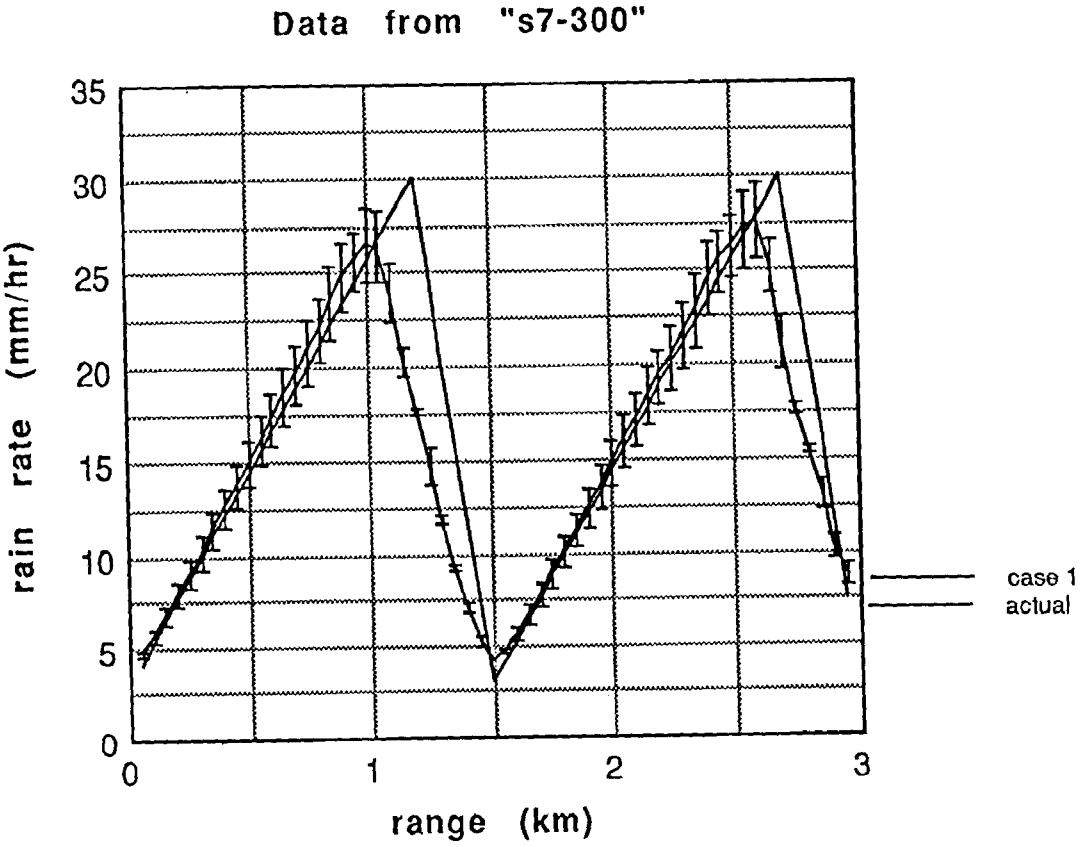
Data from "s7-300"
rain rate (mm/hr)
35
30
25
20
15
10
5
0
0
1
2
3
range (km)
case 1
actual

Figure 6

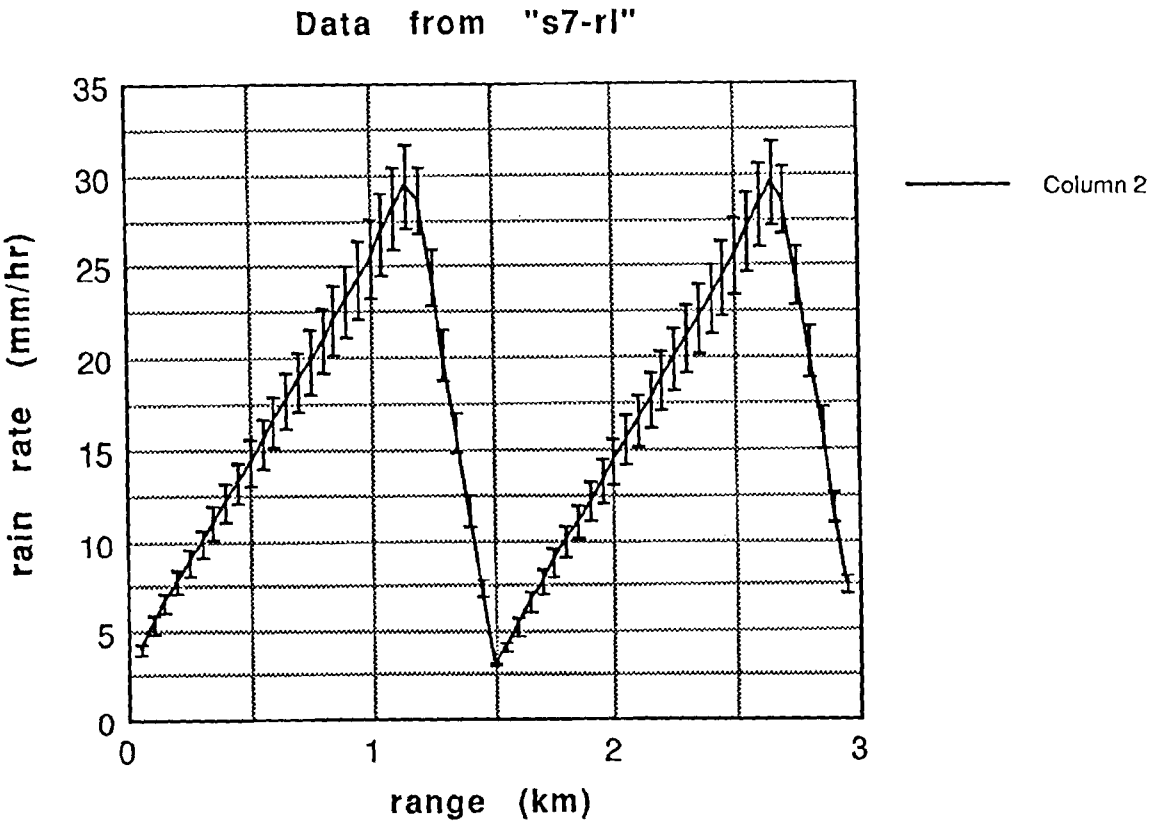
Data from "s7-rl"
rain rate (mm/hr)
35
30
25
20
15
10
5
0
0
1
2
3
range (km)
Column 2

Figure 7

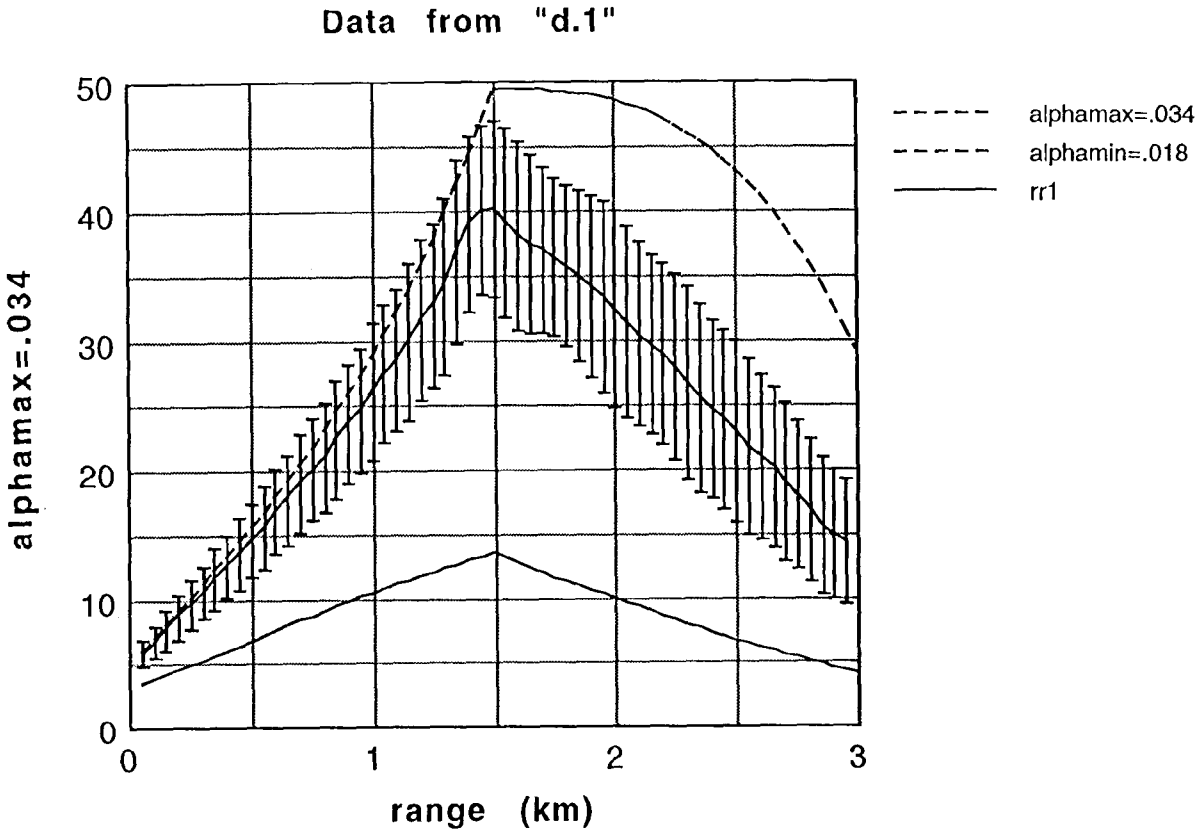
Data from "d.1"
alphamax=.034
50
40
30
20
10
0
0
1
2
3
range (km)
alphamax=.034
alphamin=.018
rr1

Figure 8

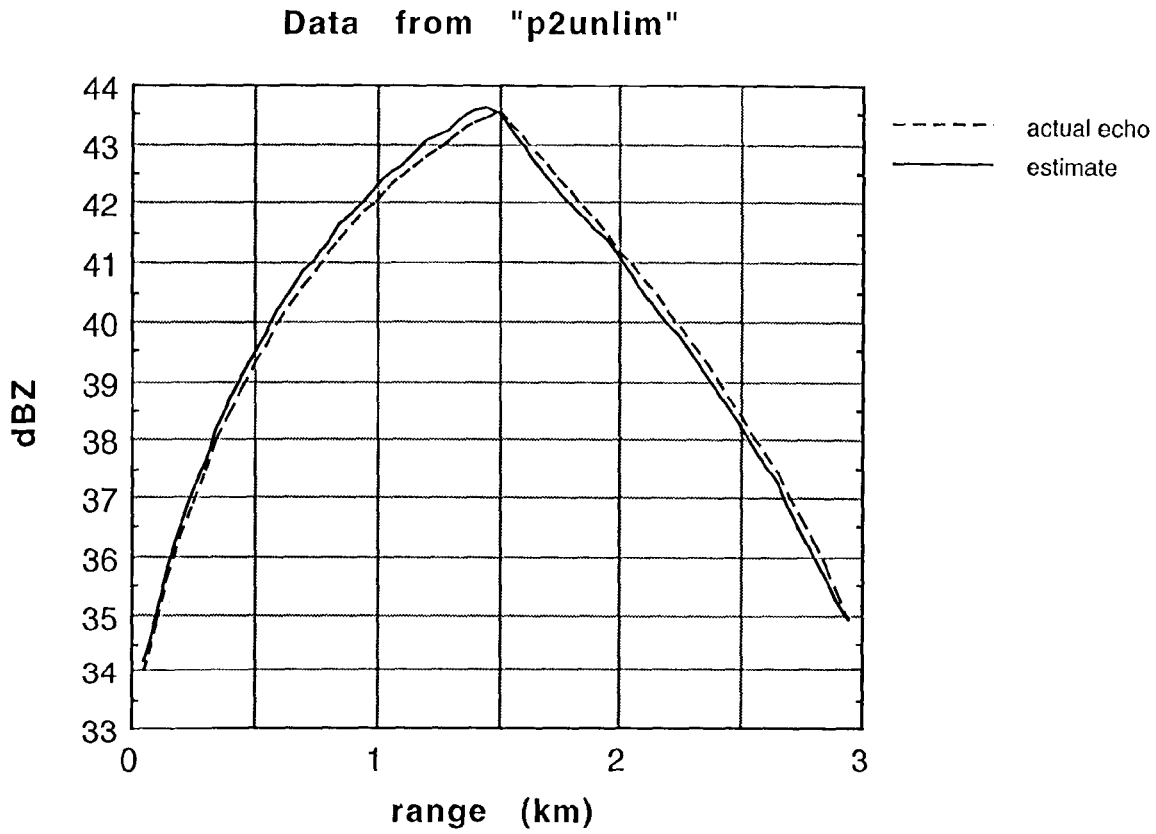
Data from "p2unlim"
dBZ
44
43
42
41
40
39
38
37
36
35
34
33
0
1
2
3
range (km)
actual echo
estimate

Figure 9

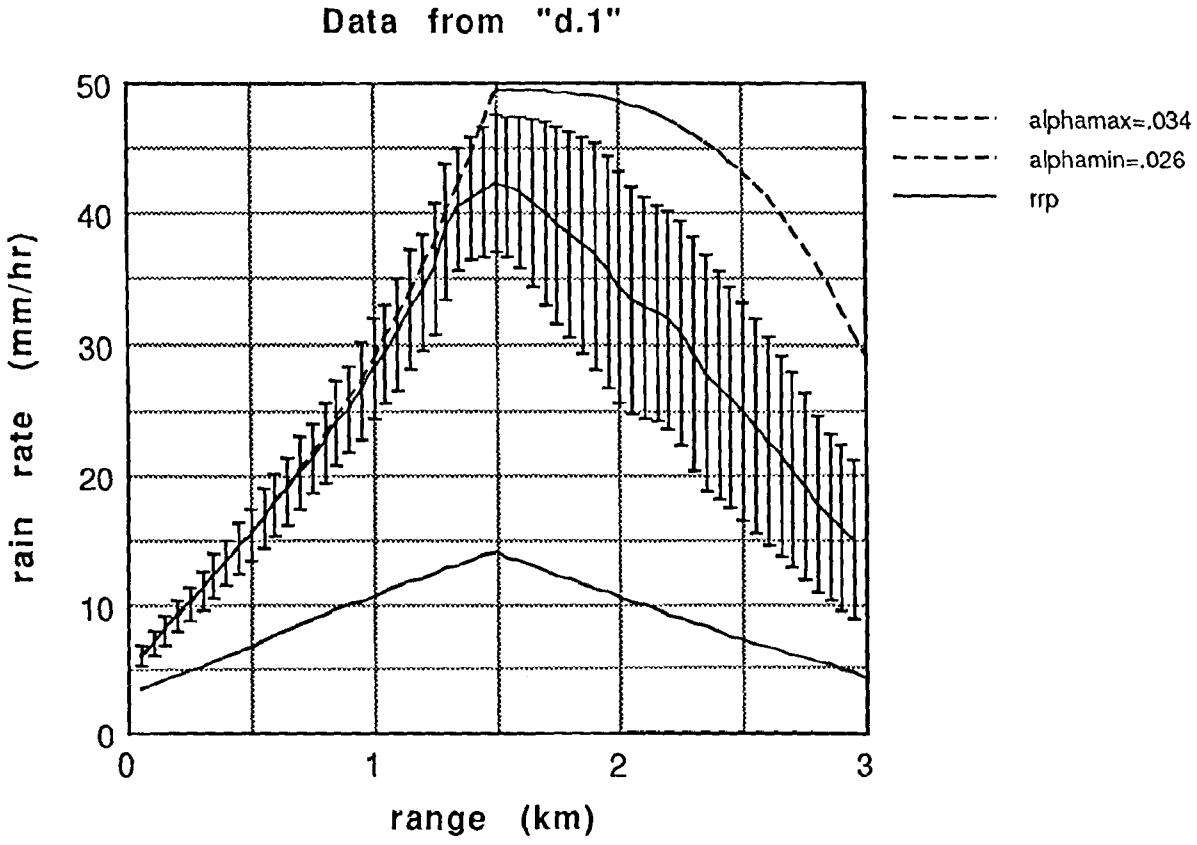
Data from "d.1"
rain rate (mm/hr)
range (km)
0
10
20
30
40
50
0
1
2
3
alphamax=.034
alphamin=.026
rrp

Figure 10

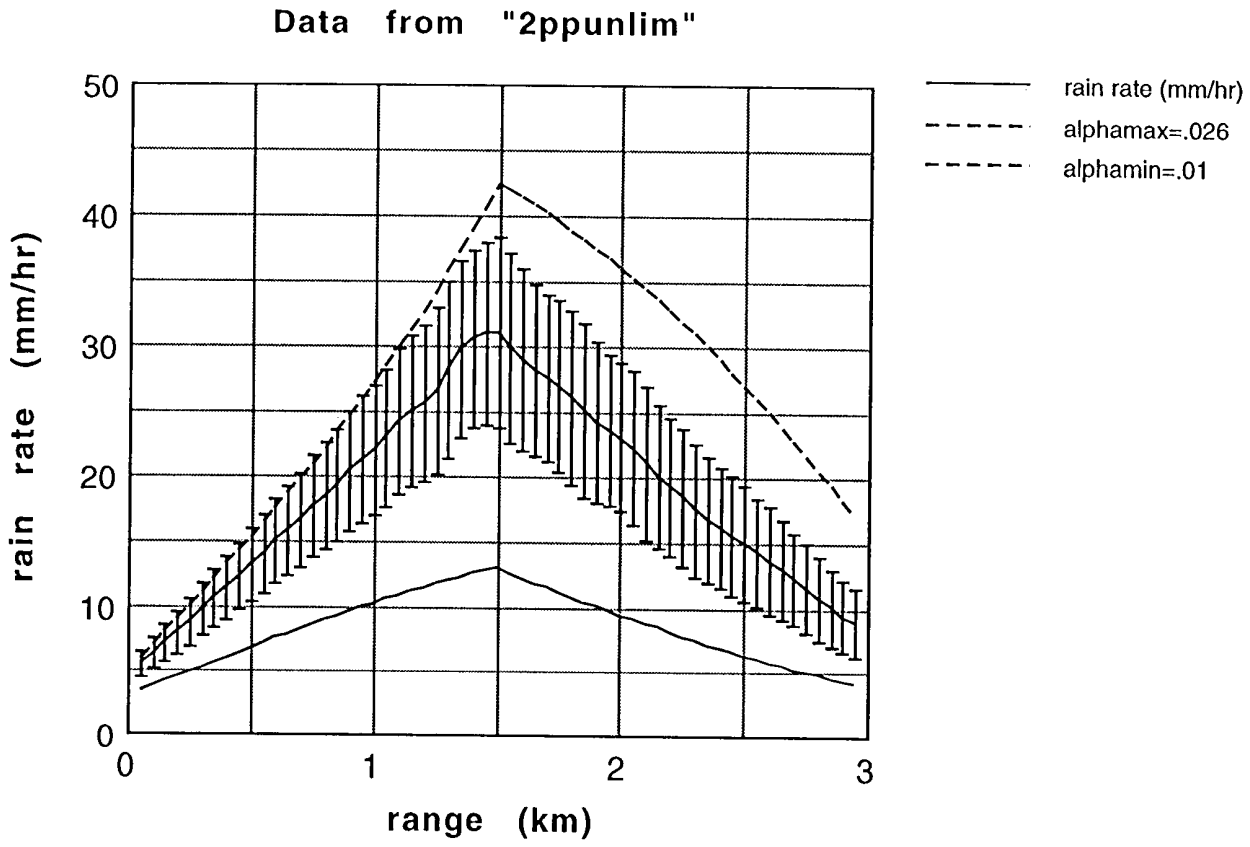
Data from "2ppunlim"
rain rate (mm/hr)
alphamax=.026
alphamin=.01
rain rate (mm/hr)
range (km)
0
10
20
30
40
50
0
1
2
3

Figure 11

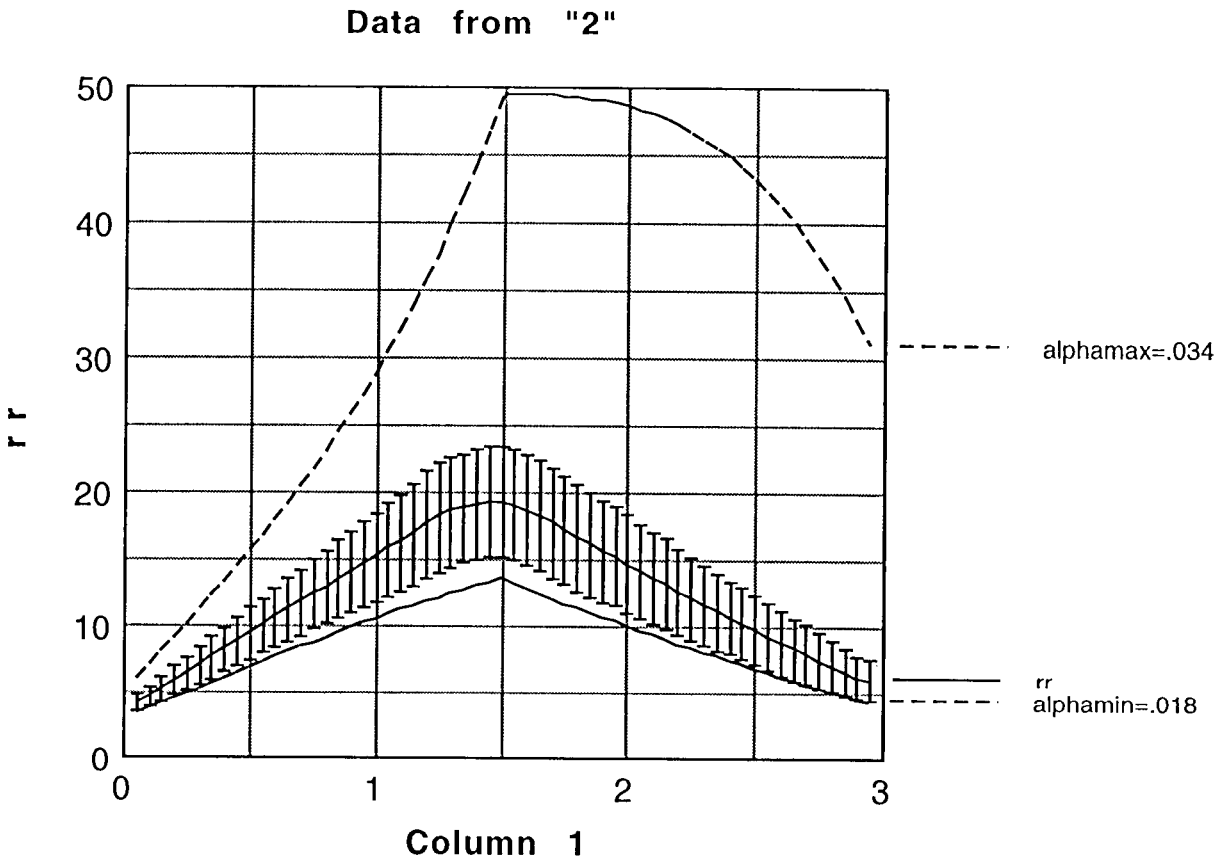
Data from "2"
50
40
30
20
10
0
r r
0
1
2
3
Column 1
alphamax=.034
rr
alphamin=.018

Figure 12

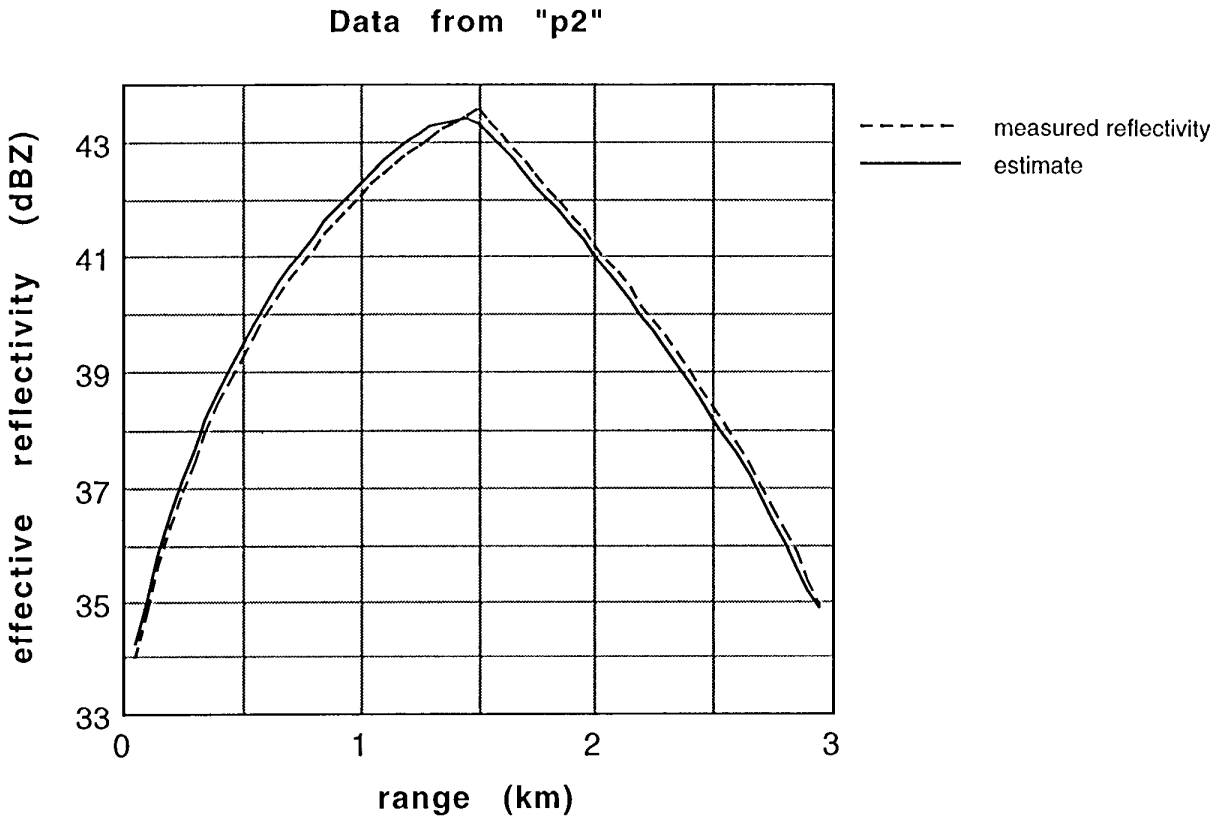
Data from "p2"
effective reflectivity (dBZ)
43
41
39
37
35
33
0
1
2
3
range (km)
measured reflectivity
estimate

13